Identification of Small-Molecule Inhibitors that Block the GTP-Binding Pocket of K-Ras and Other Members of the Ras Superfamily of Small GTPases

Luca Carta[1,†], Rebecca Hutcheson[1], Carolina L. Bigarella[1], Sufang Zhang[1], Simon A. Davis[2], Michael J. Rudolph[2], Charles H. Reynolds[3], Matthias Quick[4,5,6], Theresa M. Williams[7], Michael Schmertzler[1], and Yaron R. Hadari[1]

ABSTRACT

RAS genes encode small GTPases essential for mammalian cell proliferation, differentiation, and survival. *RAS* gene mutations are associated with 20% to 30% of all human cancers. Based on earlier reports of extremely high Ras binding affinities for GTP, Ras proteins were previously considered undruggable. Using three independent techniques, we report binding affinities of K-Ras and several K-Ras mutants for GTP in the 250 to 400 nmol/L range, orders of magnitude lower than previously reported (~10 pmol/L). This discovery suggests that K-Ras and other small-GTPase proteins may indeed be druggable targets. We identified more than 400 small molecules that compete non-covalently with GTP binding to K-Ras. Focusing on two inhibitors, we demonstrate the inhibition of K-Ras in downstream signaling and cellular proliferation in human pancreatic and non–small cell lung cancer cells expressing wild-type or mutant K-Ras. These two compounds represent novel pan-Ras superfamily inhibitors as they also inhibited GTP binding to other members such as RAB5A and RAB35.

Introduction

Ras proteins, encoded by three ubiquitously expressed genes (*HRAS*, *KRAS*, and *NRAS*; ref. 1), couple cell surface receptors to intracellular effector pathways, regulating cellular growth and differentiation (2, 3).

Ras cycles between "on" and "off" states via GTP/GDP binding, a process regulated by guanine nucleotide exchange factors which promote Ras activation via GDP release and GTP binding and GTPase-activating proteins which accelerate Ras-mediated GTP hydrolysis (2, 4–6). More than 150 human proteins belong to the Ras GTPase superfamily of small GTPases including Ras, Rac-1, Rho-A, and cdc42 that share significant homology in their GTP-binding site (7, 8). Approximately 20% to 30% of all human cancers are associated with mutations in Ras proteins (9–11), with K-Ras being the most frequently mutated isoform, particularly in pancreatic, colorectal, and lung tumors (9, 10, 12). The most frequent K-Ras mutations involve substitutions of Gly12, Gly13, and Gln61 (10, 13). N-Ras is mutated in about 20% of all patients with melanoma (14), and H-Ras mutations are comparatively rare (9). A serious unmet medical need persists for patients with diseases, such as cancer, fibrosis, and inflammatory conditions, associated with mutated *RAS* genes. Two small molecules (sotorasib and adagrasib) that covalently bind the free thiol group of the K-Ras^{G12C} mutant in the GTP/GDP-bound state and stabilize the protein in an inactive conformation have recently been approved for therapeutic applications by the FDA. Other similar covalent binders are currently in clinical development (15, 16).

However, small molecules targeting the GTP-binding site of wild-type (WT) or mutant versions of other Ras proteins, or non-covalent binders to the GTP-binding site of the K-Ras^{G12C} mutant, have not been published or proposed for clinical development.

This is likely due to the widely accepted presumption, based on studies from the 1980s and 1990s, which states that small-molecule drugs cannot compete with guanine nucleotides binding to Ras proteins (17, 18). These publications reported a calculated GTP dissociation constant (K_d) with H-Ras (referred to as p21 in the original articles) in the range of 0.6 to 55.6 pmol/L, leading to characterization of Ras GTP-binding sites as undruggable.

For the present study, we produced nucleotide-free K-Ras and several K-Ras mutants and measured their K_ds of binding to GTP. These measurements were made using three well-validated techniques: microscale thermophoresis (MST; ref. 19), scintillation proximity assay (SPA; refs. 20, 21), and a filtration binding assay. The K_ds measured for GTP and K-Ras binding were in the range of 250 to 400 nmol/L—five orders of magnitude larger than previously reported for H-Ras three decades ago (18, 22, 23), thus suggesting that the GTP-binding site of K-Ras may be susceptible to the development of non-covalently bound therapeutics.

To test the possibility of developing small-molecule competitors for GTP binding to K-Ras, we developed a novel cell-free competitive binding assay and screened a focused library of 21,500 small molecules. We identified more than 400 small-molecule competitors, representing several different core structures, which compete with GTP binding to K-Ras. We tested the ability of each of these

[1]SHY Therapeutics, LLC, Valhalla, New York. [2]New York Structural Biology Center, New York, New York. [3]GFree Bio, LLC, Austin, Texas. [4]Department of Psychiatry, Columbia University Vagelos College of Physicians and Surgeons, New York, New York. [5]Department of Physiology and Cellular Biophysics, Columbia University Vagelos College of Physicians and Surgeons, New York, New York. [6]Area Neuroscience - Molecular Therapeutics, New York State Psychiatric Institute, New York, New York. [7]Wise Consulting, LLC, Harleysville, Pennsylvania.

L. Carta and R. Hutcheson contributed equally to this article.

†Deceased

Corresponding Author: Yaron R. Hadari, SHY Therapeutics, LLC, 7 Dana Road, Suite 106, Valhalla, NY 10595. E-mail: yaron.hadari@shytherapeutics.com

Mol Cancer Ther 2025;XX:XX–XX

doi: 10.1158/1535-7163.MCT-24-0618

molecules to block K-Ras signaling and inhibit cell proliferation in several tumor-derived human cell lines. Based on these data, we selected a subset for further Structure-Activity Relationship refinement. We report here on the inhibitory activity of two of these compounds in both cell-free and cell-based assays against WT and several K-Ras mutants including G12C, G12D, G12S, and N-Ras^{Q61K}.

Materials and Methods

Cell lines

NCI-H1975 (RRID: CVCL_UE30) female, A549 (RRID: CVCL_0023) male, NCI-H1299 (RRID: CVCL_0060) male, PANC-1 (RRID: CVCL_0480) male, MIA-PaCa-2 (RRID: CVCL_HA89) male, BxPC3 (RRID: CVCL_0186) female, NIH-3T3 (RRID: CVCL_0594) male, HEK293T (RRID: CVCL_0063) female, and human dermal fibroblasts (PCS-201-012) male were purchased from ATCC and grown in ATCC-recommended complete medium supplemented with penicillin (100 U/mL) and streptomycin (100 μg/mL) at 37°C in a humidified incubator with 5% CO_2. Cell passages five to 15 were used for all experiments. *Mycoplasma* testing and cell line authentication were not performed.

Antibodies

Antibodies used were rabbit mAb anti–human phospho-EGF receptor (Tyr1068; RRID: AB_2096270), rabbit mAb anti–human EGFR (RRID: AB_2246311), rabbit mAb anti–human phospho-AKT (Ser473; RRID: AB_2315049), rabbit mAb anti–human pan-AKT (RRID: AB_2225340), rabbit mAb anti–human phospho-p44/42 ERK (Thr202/Tyr204; RRID: AB_331772), rabbit Ab anti–human p44/42 ERK (RRID: AB_330744), rabbit Ab anti–human phospho-MEK1/2 (Ser217/221; RRID: AB_331648), rabbit mAb anti–human MEK1/2 (RRID:AB_331778), and mouse mAb anti–human RAS (Cell Signaling Technology).

Compounds

SHY-855 (100% purity) and SHY-867 (97% purity) were synthesized at Enamine LLC. Experimental details for the synthesis of the compounds can be found in patent WO2020132071 (24). SHY-855 is Example 40 and SHY-867 Example 21.

Recombinant proteins

K-Ras (residues 2–185), Rac-1 (residues 1–177), Rho-A (residues 2–181), RAB5A (residues 1–215), and RAB35 (residues 1–201) were subcloned into the MCSG7 bacterial expression vector encoding an N-terminal deca-histidine fusion tag with a TEV protease cleavage site. All proteins were expressed in *Escherichia coli* BL21(DE3) Gold cells and purified by nickel affinity and size-exclusion chromatography on an AKTAxpress system (GE Life Sciences), consisting of a 1-mL nickel affinity column, followed by a Superdex 200 16/60 gel filtration column. The final protein buffer consisted of 50 mmol/L Tris-HCl pH 7.5, 150 mmol/L NaCl, 1 mmol/L $MgCl_2$, and 1 mmol/L dithiothreitol (buffer I).

Kinetic studies

MST experiments were performed according to the NanoTemper Technologies protocol in a Monolith NT.115 (red) instrument (NanoTemper Technologies). Binding was measured with 40 nmol/L EDA-GTP-Cy5 or -Cy3 (Jena Bioscience GmbH) and His-tagged labeled proteins (0.68 nmol/L–11 μmol/L) in buffer I. Data analyses and K_d calculation were performed using MO.Affinity Analysis software (NanoTemper Technologies).

SPAs were performed using 25 ng purified recombinant protein immobilized on 1.25 mg copper-coated His-tag SPA beads per mL of assay buffer (20 mmol/L Tris-Cl, pH 7.45, 150 mmol/L NaCl, 3 mmol/L $MgCl_2$, and 1 mmol/L Tris (2-carboxy-ethyl)-phosphine-HCl) in 100 μL assays. In pilot experiments, 25 ng was determined to prevent radioligand depletion and yield a level of protein occupation far below the binding capacity of the beads. YSi (yttrium silicate) copper-coated His-tag beads (PerkinElmer) were used in combination with a [^{32}P]GTP (American Radiolabeled Chemicals, Inc.; 3,000 Ci/mmol). All binding assays were performed in 96-well white wall clear-bottom plates and assayed in the Wallac photomultiplier tube MicroBeta counter. Saturation binding experiments were performed with increasing concentrations of radiolabeled GTP (2.5 nmol/L–10 μmol/L), and nonspecific binding (the non-proximity signal) was assayed with 800 mmol/L imidazole. The stoichiometry of radiolabeled GTP binding to GTPases was determined by using known amounts of protein (1.2 pmol) and calculating the specific binding (total signal – non-proximity signal) at each tested GTP concentration. Counts per minute were transformed into pmol using known concentrations of radiolabeled GTP to determine the efficiency of detection. Non-linear regression fitting in GraphPad Prism 7 was used to calculate the K_d and maximum binding (B_{max}) by plotting the bound pmol of GTP as a function of free GTP. Knowing the 1:1 stoichiometry of GTP and Ras binding, and using a known amount of protein, K_d represented the concentration of α-[^{32}P]GTP at 50% of B_{max}.

Data were generated from three independent experiments performed with technical triplicates.

Filtration binding assay: binding was performed with varying amounts of protein for 5 minutes at 23°C in 100 μL assays using a final concentration of 2.88 nmol/L α-[^{32}P]GTP (2,594 Ci/mmol; PerkinElmer). Samples were filtered through 0.45-μm nitrocellulose filters, type BA85 (Whatman) or comparable nitrocellulose filters from Millipore (MF-Millipore; 0.45-μm MCE membrane), and filters were washed with ice-cold assay buffer without GTP. Dried filters were counted in the Hidex 300 SL scintillation counter to determine the disintegrations per minute.

Cell-free assay for GTP-binding proteins

Purified His-tagged proteins were diluted to 3 to 10 μg/mL in 1X TBS containing 1 mmol/L $MgCl_2$ and 1 mmol/L dithiothreitol (buffer I). To a nickel-coated 96-well plate, 200 μL of the protein suspension was added and incubated for 1 hour at 23°C . Molecules were added to the protein-coated wells at final concentration of 20 μmol/L. For IC_{50} measurements, serial dilutions were prepared and added to the protein-coated wells. Following 3 hours of incubation at 23°C, Cy3-GTP or Cy5-GTP was added to each well in a final concentration of 100 nmol/L. The labeled GTP was incubated for 45 minutes at 23°C. Wells were washed 3× in buffer I, and 200 μL of buffer I was added to each well and bound labeled GTP was measured with a Molecular Devices SpectraMax M3 plate reader.

Cell-based phosphorylation assays

Cells were plated at 350,000 cells/well density in a 12-well plate, allowed to adhere for 3 hours, and then starved in the appropriate medium in the presence of 0.5% FBS overnight. Serial dilutions of molecules were added to cells in the presence of 0.3% DMSO for 6 hours at 37°C. Next, cells were stimulated with 1.5 ng/mL EGF for 15 minutes and then lysed with buffer containing 1% Triton X-100, EDTA, and Halt Protease and Phosphatase Inhibitor

Cocktail (Thermo Fisher Scientific). Protein concentration was assessed by bicinchoninic acid protein assay (Thermo Fisher Scientific).

Western blotting

Equal volumes of eluate (25 μL) were separated by 10% SDS-PAGE and transferred to nitrocellulose membranes (Invitrogen by Thermo Fisher Scientific). The membrane was stained with Ponceau S Stain (Boston BioProducts) to verify uniform protein loading. Membranes were blocked with 5% BSA in Tris Buffered Saline-Tween-20 and then incubated overnight at 4°C with primary antibody, followed by horseradish peroxidase–conjugated secondary antibody (Jackson ImmunoResearch). Membranes were incubated in Amersham ECL Prime Western Blotting Detection Reagent (GE Healthcare) and visualized using the ChemiDoc MP imaging system (Bio-Rad). Image Lab 6.1 (Bio-Rad) was used for Western blot densitometry measurements. p-ERK1/2, p-AKT, and p-MEK1/2 bands were normalized to the corresponding total protein levels. Percent inhibition was calculated using the equation 100−[(phosphorylated sample/phosphorylated EGF + control)/(total sample/total EGF + control) × 100].

cAMP assay

Cells were seeded at a density of 8,000 cells per well in a 96-well white plate with a clear bottom and allowed to grow overnight. The following day, cells were treated with either 1.0 μmol/L SHY-855, 1.0 μmol/L SHY-867, or DMSO for 1 hour. The cAMP assay was performed using the cAMP-Glo Assay Kit (Promega) according to the manufacturer's protocol. Luminescence was measured using a SpectraMax M3 plate reader.

GTP pull down assay

Cells were plated at 2×10^6 cells/well density in a six-well plate, allowed to adhere for 3 hours, and then starved in the appropriate medium containing 0.5% FBS overnight. Serial dilutions of the small molecules to be tested were added to the cells in the presence of 0.3% DMSO for 6 hours of incubation at 37°C. Next, cells were stimulated with 1.5 ng/mL EGF for 15 minutes, rinsed with ice-cold PBS, and lysed with 200 μL of lysis/binding/wash buffer from the Active Ras Detection kit (Cell Signaling Technology, #8821) supplemented with phenylmethylsulfonyl fluoride (Sigma). An aliquot of the lysate was reserved for protein quantification and the rest of the lysate was snap frozen. Protein concentration was determined by bicinchoninic acid protein assay (Thermo Fisher Scientific). Following the manufacturer's instructions, 500 μg of the lysate was incubated with 32 μg of GST-RAF1-RBD to pull down RAS-GTP. Lastly, samples were eluted from GST beads, fractionated on 4% to 20% SDS-PAGE, and analyzed by Western blotting using a pan RAS antibody contained in the kit.

Proliferation assay

Cells were plated at 4,000 cells/well in a 96-well plate. The next day, serial dilutions of the molecules were added in the presence of 0.3% DMSO and 10% FBS. Cells were then incubated for 3 days at 37°C in a humidified incubator with 5% CO_2. Cell viability was determined using the CellTiter 96 AQueous One Solution Cell Proliferation Assay according to manufacturer's specifications (Promega).

Statistical analysis

All IC_{50} calculations were performed by nonlinear regression using the GraphPad Prism software.

Results

GTP affinity to WT K-Ras and three K-Ras mutants

We first used MST to measure the K_d of GTP binding to WT K-Ras, three K-Ras mutants (G12D, G12C, and Q61H) that are the predominant forms of mutated K-Ras found in human tumors, and two other Ras family members, Rac-1 and Rho-A (**Table 1**; Supplementary Fig. S1). The measured K_d for WT K-Ras by MST was 460 nmol/L. The measured K_d values for the three tested K-Ras mutants were in a range of 157 to 244 nmol/L. For reference, as indicated in **Table 1** and Supplementary Fig. S1, the measured K_d for GTP binding by Rac-1 was 166 nmol/L by MST and 130 nmol/L for Rho-A. Our data are comparable with the data reported by Zhang and colleagues (25) using a filtration assay in which Rac-1 and Rho-A exhibited K_ds for GTP binding of 240 and 160 nmol/L, respectively.

We also performed SPA-based binding assays with radiolabeled GTP and filtration binding assays similar to those used in the original publications (17, 18, 21) to measure the binding constants K_d, k_{on}, and B_{max}. SPA is an established method that directly measures high-affinity ligand–protein interactions utilizing radiolabeled ligands and immobilized protein targets (20, 26). It is well suited to generating K_d and k_{on} measurements and has been used extensively in drug discovery and high-throughput screening of chemical libraries (27, 28). We prepared the proteins for the SPA and filtration binding studies with the same methods used for the MST studies. **Table 1** presents the affinities we measured by SPA for K-Ras WT, the three K-Ras mutants tested by MST, and Rac-1 and Rho-A.

The measured K_d for WT K-Ras by SPA was 246 nmol/L, roughly half the value measured by MST. The measured K_d values for the three tested K-Ras mutants were in a range of 118 to 280 nmol/L. The measured K_d for GTP binding by Rac-1 was 151 nmol/L and of Rho-A 129 nmol/L, both within an SD of the measurements made by MST. These values are comparable with those measured by us by MST and also as reported by Zhang and colleagues(25). The measured B_{max} values in **Table 1** obtained by SPA and filtration assay indicate a molar binding stoichiometry of GTP to target protein of unity, confirming that all tested recombinant proteins were purified in nucleic acid–free form.

Supplementary Table S1 presents the k_{on} measurements by SPA for WT K-Ras ($3.22 \times 10^8\ M^{-1}\ s^{-1}$) and the three K-Ras mutants ($1.88 - 6.35 \times 10^8\ M^{-1}\ s^{-1}$), as well as for Rac-1 and Rho-A. The Ras family member k_{on} measurements, including of the mutants, are all within a factor of 10 of one another.

Finally, using α-[^{32}P]GTP in a saturation filtration binding experiment (**Table 1**; Supplementary Fig. S2), we determined K_d for the binding of GTP to K-Ras and the G12D K-Ras mutant and, in a standard time course study, the k_{on} for those proteins as well. As presented in **Table 1** and Supplementary Table S1, the K_d value measured for K-Ras in the filtration binding assay was 228 nmol/L and for the G12D K-Ras mutant, 345 nmol/L. The k_{on} value measured for K-Ras was $2.13 \times 10^8\ M^{-1}\ s^{-1}$ and for the G12D K-Ras mutant was $2.49 \times 10^8\ M^{-1}\ s^{-1}$. These values are all within a factor of two of those measured by MST and SPA.

The current studies were based on purified nucleotide-free K-Ras proteins generated in a manner different than used in the

Table 1. K_d and B_{max} values of GTP and GDP binding to several members of the Ras superfamily of small GTPases obtained by filtration assay, MST, and SPA (nmol/L).

	MST	MST	SPA		Filtration assay	
Protein	**GTP K_d**	**GDP K_d**	**GTP K_d**	**B_{max} (mol:mol)**	**GTP K_d**	**B_{max} (mol:mol)**
K-Ras (WT)	463 ± 23	394 ± 54	246 ± 19	1.00 ± 0.01	228 ± 26	0.93 ± 0.03
K-Ras (G12D)	244 ± 12		280 ± 19	0.97 ± 0.01	345 ± 25	0.95 ± 0.02
K-Ras (G12C)	207 ± 46	360 ± 34	359 ± 35	0.94 ± 0.02		
K-Ras (Q61H)	157 ± 21		118 ± 11	0.96 ± 0.02		
Rac-1	166 ± 10		151 ± 14	1.03 ± 0.02		
Rho-A	130 ± 5		129 ± 12	1.02 ± 0.02		

publications from the 1980s and 1990s (29). There the expressed H-Ras protein was incubated for 40 minutes during the exchange protocol. In addition, the resulting proteins were thermally unstable and thus experiments were conducted predominantly at 0, 5, and 10°C. We generated nucleotide-free protein based on routine affinity chromatography (see "Materials and Methods"). Current experiments were conducted at 23°C and the proteins were confirmed to be stable for the time frame in which experiments were conducted. After 72 hours of incubation at 4°C, only a limited reduction in K-Ras protein activity was detected (Supplementary Fig. S3). The Q61H mutant lost 5% activity, the WT and G12D mutants lost 25% activity, and the G12C mutant lost 40% activity.

The previous publications by Feuerstein and colleagues (17), Jones and colleagues (18), and Goebel and colleagues (23) reported K_d values based on measurements of k_{on} and k_{off}. The measured k_{on} values in these three publications were 2.90×10^6 $M^{-1}s^{-1}$, in the range of $1.7 - 2.8 \times 10^5$ $M^{-1}s^{-1}$ to 4.22×10^6 $M^{-1}s^{-1}$, respectively. The measured k_{off} values in the three publications were 8.0×10^{-5}-s^{-1}, in the range of 10–156 $\times$ 10^{-8} s^{-1} to 1.1×10^{-5} s^{-1}, respectively, implying mean lives of 10^2 to 10^5 minutes. Accordingly, the calculated K_d for the binding of GTP by H-Ras was 16.7 pmol/L as reported by Feuerstein and colleagues and in the range of 0.6 to 55.6 pmol/L as reported by Jones and colleagues. The calculated K_d for the binding of GDP by K-Ras was reported by Goebel and colleagues to be 2.5 pmol/L.

To put these previously reported figures in perspective relative to the values reported here, the previously measured k_{on} values (17, 18, 23) range over a factor of 10 and are 102 to 103 greater than our SPA- and filtration-based binding measurements. The previously measured k_{off} values range over a factor of 10^3 and differ by a factor of 10^{-5} to 10^{-9}, respectively, relative to the k_{off} values reported here that were calculated algebraically from our K_d and k_{on} measurements. The resulting calculated K_d values in these two publications are therefore factors of 10^4 to 10^6 lower than the values we measured by MST, SPA, and filtration binding assays.

Development of a novel GTP competition assay

The affinity data presented in **Table 1** led us to conclude that the GTP-binding site in members of the Ras superfamily could

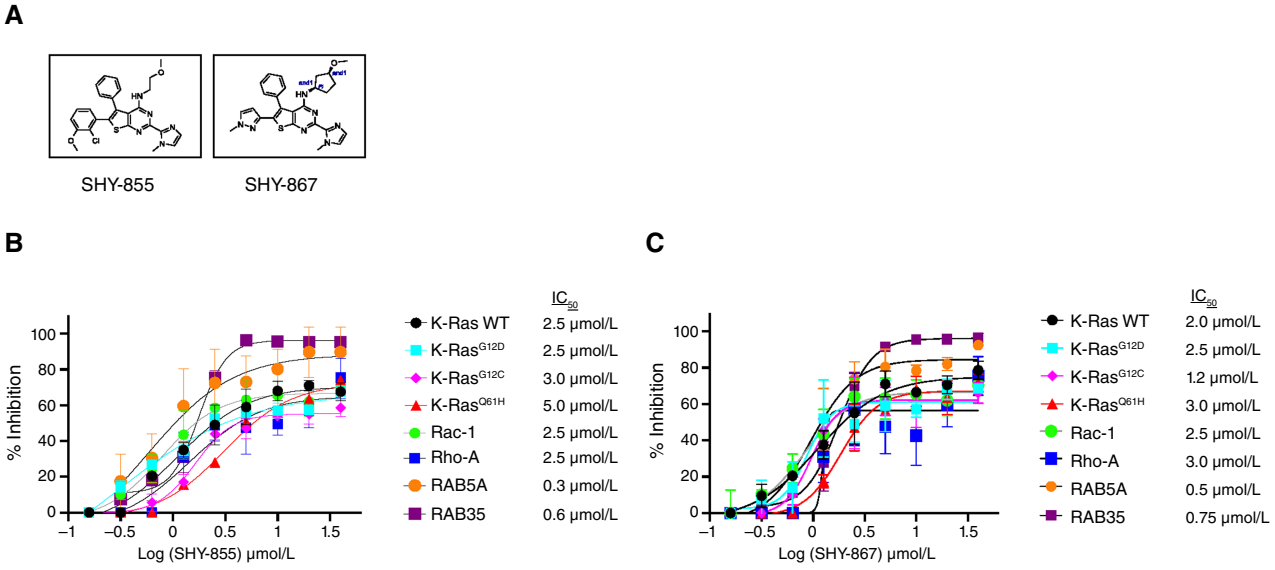

Figure 1.

Two selected molecules compete for the GTP-binding site of K-Ras proteins and other members of the Ras superfamily of small GTPases. **A,** Chemical structures of compounds SHY-855 and SHY-867. IC_{50} curves of the tested compound SHY-855 (**B**) and SHY-867 (**C**) blocking binding of 100 nmol/L fluorescent-labeled GTP to different K-Ras proteins and other members of the Ras superfamily of small GTPases.

potentially serve as a target for small molecule drug development. We hypothesized that blocking GTP binding to Ras with a small molecule could render Ras in an inactive conformation, similar to the GDP-bound conformation, blocking signaling along downstream pathways and thereby exerting a therapeutic benefit.

To identify small molecules that bind to the GTP-binding site of WT and mutant Ras proteins, we developed a 96-well cell-free competitive binding assay with which we screened a focused library of approximately 21,500 small molecules. The assay measured the ability of small molecules to compete with the binding of fluorescently (Cy3 or Cy5) labeled GTP to immobilized recombinant Ras ("Materials and Methods"). Each plate contained control wells with or without unlabeled GTP and the calculated *Z*-value of each plate was > 0.45.

Utilizing this competitive binding assay, from the starting focused library, we identified more than 400 compounds that compete with GTP for binding to K-Ras WT and the K-Ras^{G12D}, K-Ras^{G12C}, and K-Ras^{Q61H} mutants. Structure analysis of these hits revealed eight different core structures.

We subsequently developed compounds around the eight core structures that robustly inhibit GTP binding to the K-Ras variants. **Figure 1** summarizes the IC_{50} as measured by the competitive binding assay of two representative compounds (referred to as SHY-855 and SHY-867) that compete with GTP binding to K-Ras WT, the G12D, G12C, and Q61H mutants, as well as Rac-1, Rho-A, Rab5, and Rab35. All proteins were expressed with His-tag in an established *E. coli* expression system (Supplementary Fig. S4). Consistent with the inference drawn from our binding studies, the IC_{50} values of these molecules demonstrate that small molecules can bind non-covalently to the GTP-binding site of Ras and competitively prevent GTP binding to that site. Interestingly, the IC_{50}s of the two tested RAB proteins were the lowest, indicating that specificity to proteins within the Ras superfamily can be achieved and that Ras proteins are not the only targets of these compounds. It should be noted that the measured IC_{50} values in the sub μM range are a function of the optimized 100 nmol/L concentration of the fluorescent-labeled GTP in the assay and are not a measure of affinities. We also tested sotorasib, adagrasib, and RMC-6236 in the GTP competition assay (Supplementary Table S2). These inhibitors were tested against WT, G12C, and G12D K-Ras. As predicted, sotorasib and adagrasib were very active on the K-Ras^{G12C} mutant, whereas adagrasib had some activity on WT K-Ras. RMC-6236 had no inhibitory effect.

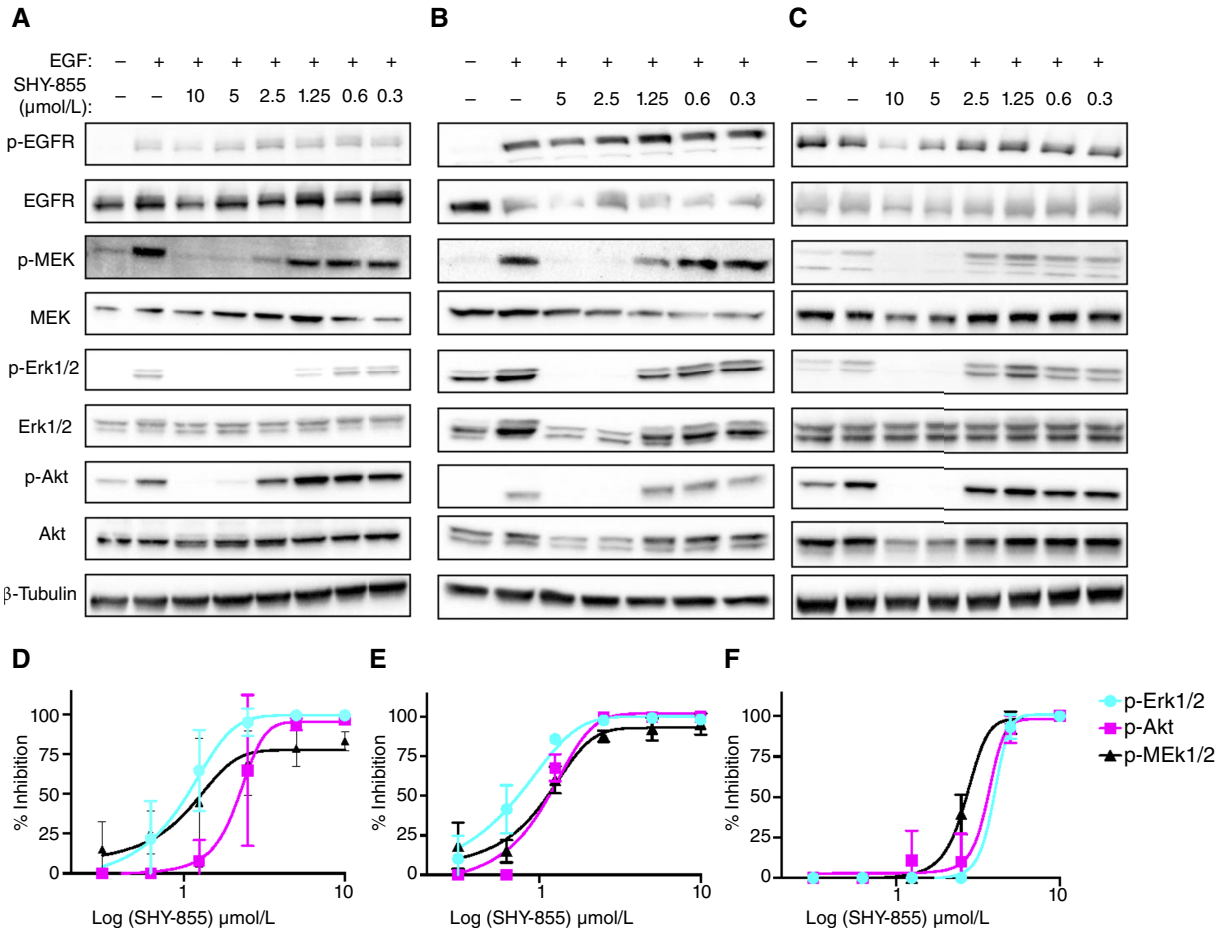

Figure 2.

Compound SHY-855 inhibits K-Ras downstream signaling. Cells were incubated with compound SHY-855 for 6 hours with the indicated concentrations, stimulated with EGF for 15 minutes, and cell lysates were analyzed using the indicated phospho-specific antibodies. **A,** PANC-1 cell line, (**B**) MIA PaCa-2 cell line, (**C**) NCI-H1975 cell line represent Western blot analysis. All experiments were performed in triplicates. **D,** Graphical presentation of densitometry measurements representing % inhibition of the triplicates in PANC-1 cells, (**E**) same in MIA Paca-2 cells, and (**F**) in NCI-H1975 cells.

Overall, the two compounds, SHY-855 and SHY-867, demonstrate similar IC_{50} values, in the range of 0.3 to 5.0 μmol/L, against the tested proteins (**Fig. 1**), suggesting they may be pan-Ras superfamily inhibitors. This may be explained by the high sequence homology of the GTP-binding sites among these proteins. In order to verify whether the two compounds may also modulate the activity of G-alpha subunits of G Protein-Coupled Receptors, we tested their effects on cellular levels of cAMP (Supplementary Fig. S5). As demonstrated in Supplementary Fig S5, the compounds did not affect cellular levels of cAMP. We thus concluded that they are most likely specific inhibitors of the Ras superfamily of small GTPases and do not interact or modulate the G-alpha subunit of G Protein-Coupled Receptors.

Inhibition of Ras downstream pathways

We tested the inhibitory effects of SHY-855 and SHY-867 on Ras-associated signal transduction pathways in three human cell lines: the pancreatic cell lines PANC-1 (K-Ras^{G12D} mutant) and MIA PaCa-2 (K-Ras^{G12C} mutant) and the non–small cell lung cancer cell line NCI-H1975 (K-Ras WT). **Figs. 2** and **3** illustrate the inhibitory effects of SHY-855 and SHY-867 on phosphorylation of MEK, Erk1/2, and Akt in those three cell lines. As shown in **Fig. 2** (and Supplementary Fig. S6), SHY-855 inhibited phosphorylation and activation of MEK, Erk1/2, and Akt in PANC-1, MIA PaCa-2, and NCI-H1975 cell lines in a dose-dependent manner with similar IC_{50} values (about 1–3 μmol/L). These effects would be expected from a Ras inhibitor that is an upstream blocker of the two pathways and support the notion that compound SHY-855 induces an inactive conformation of Ras through a consistent binding mode, regardless of mutation. In contrast, the IC_{50}s of SHY-867 on the phosphorylation of MEK and Erk1/2 were approximately 1 μmol/L in PANC-1 and MIA PaCa-2 and 5 μmol/L in NCI-H1975 and were approximately 7 μmol/L in PANC-1 and MIA PaCa-2 and 10 μmol/L in NCI-H1975 for Akt (**Fig. 3**; Supplementary Fig. S7). These data suggest a differential downstream signaling effect requiring further study.

Inhibition of the Ras–GTP complex

As a follow up to our downstream assays, we also measured the ability of SHY-855 and SHY-867 to inhibit Ras–GTP complex formation in the three cell lines (PANC-1, MIA PaCa-2, and

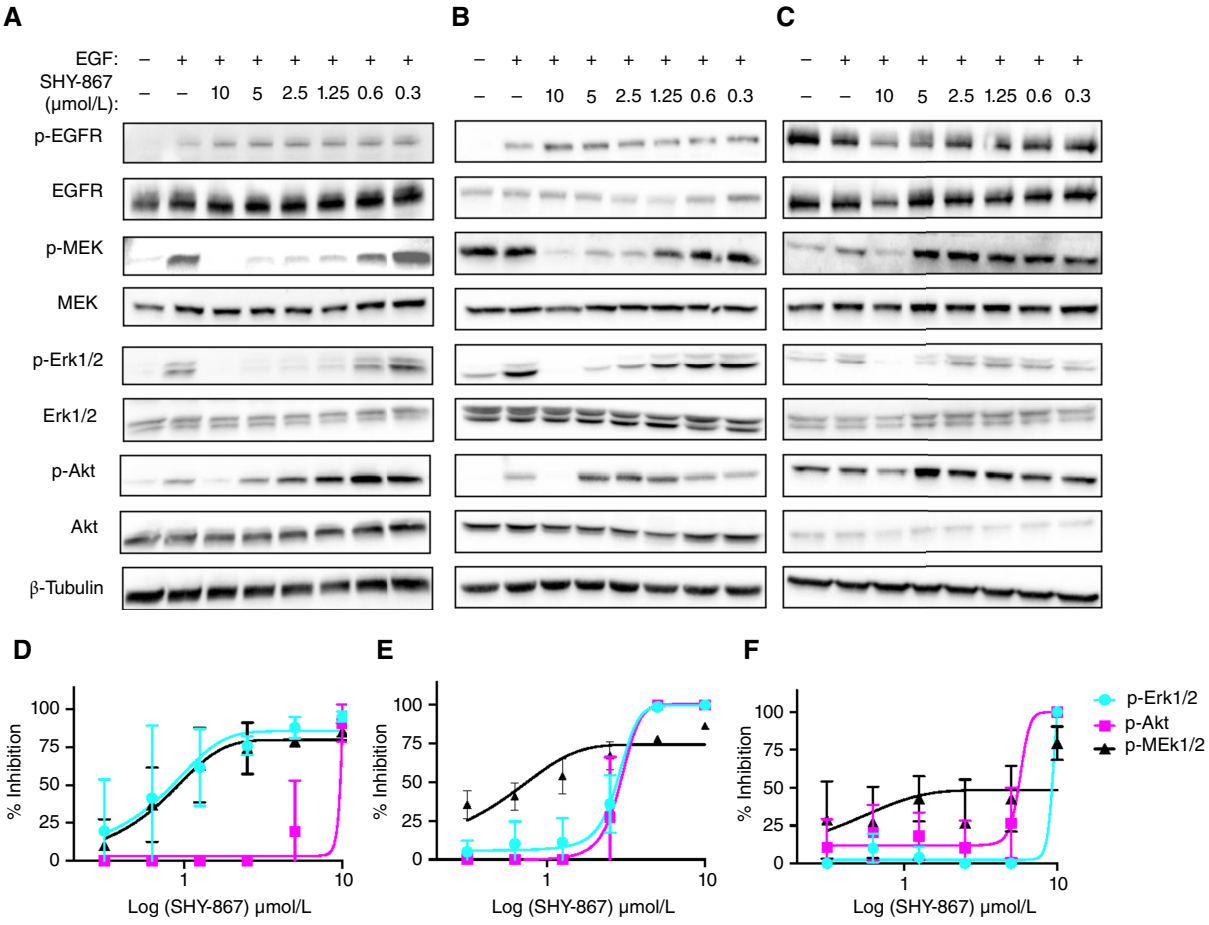

Figure 3.

Compound SHY-867 inhibits K-Ras downstream signaling. Cells were incubated with compound SHY-867 for 6 hours with the indicated concentrations, stimulated with EGF for 15 minutes, and cell lysates were analyzed using the indicated phospho-specific antibodies. **A,** PANC-1 cell line, (**B**) MIA PaCa-2 cell line, (**C**) NCI-H1975 cell line represent Western blot analysis. All experiments were performed in triplicates. **D,** Graphical presentation of densitometry measurements representing % inhibition of the triplicates in PANC-1 cells, (**E**) same in MIA Paca-2 cells, and (**F**) in NCI-H1975 cells.

NCI-H1975) using a Ras pull-down assay ("Materials and Methods"). As shown in **Fig. 4**, both compounds prevent Ras–GTP complex formation with IC_{50} values in the range of 1 to 3 μmol/L. These values correlate well with the IC_{50} values obtained for the inhibition of MEK, Erk1/2, and Akt phosphorylation presented in **Figs. 2** and **3**. This inhibition of Ras–GTP complex formation strongly suggests that both compounds bind directly to the GTP-binding site of Ras and induce a Ras inactive conformation, similar to the GDP-bound state.

Anti-proliferative effects induced by the two selected compounds

We further measured the inhibition of SHY-855 and SHY-867 on cellular proliferation in several cell lines: the three cell lines mentioned above in the signaling studies (PANC-1, MIA PaCa-2, and NCI-H1975), the pancreatic cell line BxPC3 (K-Ras WT), the non–small cell lung cancer lines A549 (K-Ras^{G12S} mutant) and NCI-H1299 (N-Ras^{Q61K} mutant), and three cell lines expressing K-Ras WT HEK293T, NIH-3T3, and human dermal fibroblast. **Figure 5** summarizes the IC_{50} values measured in these studies. Molecules SHY-855 and SHY-867 both inhibit cellular proliferation in a dose-dependent manner with similar IC_{50} values, ranging from approximately 0.3 to 2.9 μmol/L in all tested cell lines. Consistent with the notion that these two compounds are pan-Ras superfamily inhibitors, it is reasonable to speculate that they can inhibit pathways downstream of several members of the Ras superfamily. Interestingly, in contrast to the different IC_{50} values obtained for inhibition of phosphorylation and activation of MEK, Erk1/2, and Akt, the IC_{50} values for inhibition of proliferation are more similar. When we tested the inhibitory effects of these two SHY compounds in combination with adagrasib in the proliferation assay in MIA PaCa-2 cells, no additive or synergistic effects were identified (Supplementary Fig. S8). These data support the notion that Ras downstream pathways are most important for proliferation, thus inhibiting it by two different compounds has no additive or synergistic effects.

Discussion

Given the substantial association of K-Ras mutations with human disease, reducing barriers to the development of therapeutics targeting the GTP-binding site of K-Ras and other members of the Ras GTPase superfamily is imperative. Motivated by several earlier publications of K_ds in the nanomolar range for members of the Ras superfamily (30–34), we conducted kinetic measurements using three validated, scientifically advanced techniques to challenge the historically accepted picomolar measurements, which led to belief that the GTP-binding site of K-Ras is "undruggable." Our results demonstrate that the development of small-molecule competitors for GTP binding to K-Ras is feasible.

The new affinity data presented here contradict the previous publications that proposed high-affinity K_ds between H-Ras and GTP in the range of 0.6 to 55.0 pmol/L (17, 18, 23). Our data are based on and consistent across three well-validated methods: MST and SPA, which were not available in 1990, and filtration binding studies, similar to those conducted three decades ago.

Our kinetic measurements were undertaken as a stepping stone to justify the work necessary to pursue the development of small-molecule competitors to GTP K-Ras binding. They were not designed to replicate the earlier measurements or to pinpoint sources of the differences between them and the new measurements reported here. Nevertheless, the question remains with regard to why the kinetic values reported previously differ so markedly from those we report from our filtration assays (as well as the MST and SPA values).

A number of factors may have combined to contribute to the differences between the previous measurements and those reported

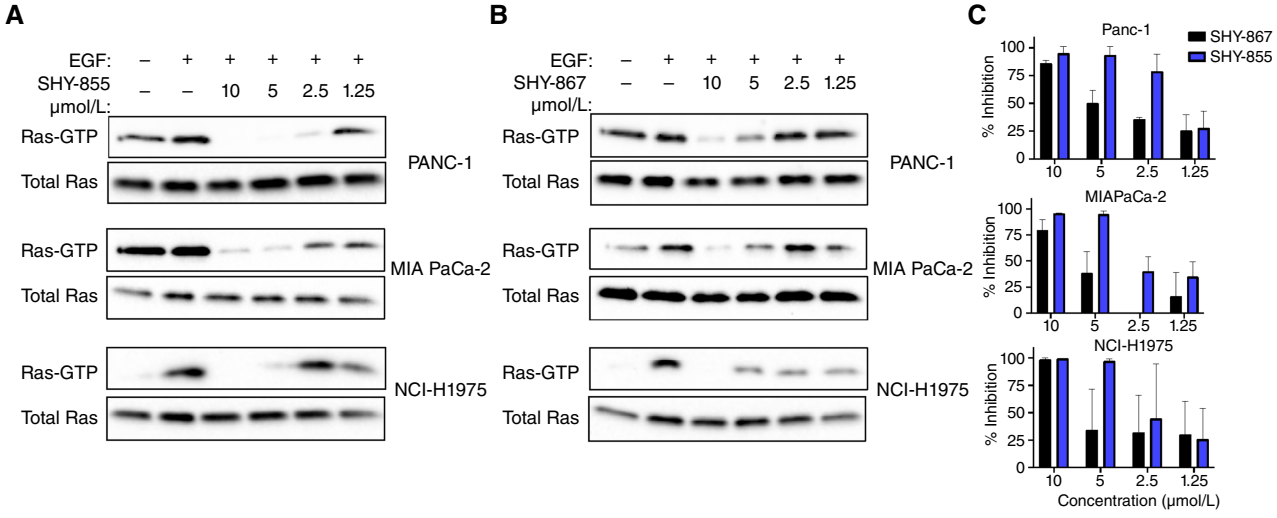

Figure 4.

Compounds SHY-855 (**A**) and SHY-867 (**B**) inhibit Ras–GTP complex formation. The indicated cell lines were incubated with compound SHY-855 or SHY-867 for 6 hours with the indicated concentrations and stimulated with EGF for 15 minutes. GTP pull down assay was performed on the cell lysates as described under "Materials and Methods." All experiments were performed in triplicates and the presented data are from one experiment of the three repeats. Graphical presentation of densitometry measurements representing % inhibition of the triplicates in the different tested cell lines (**C**).

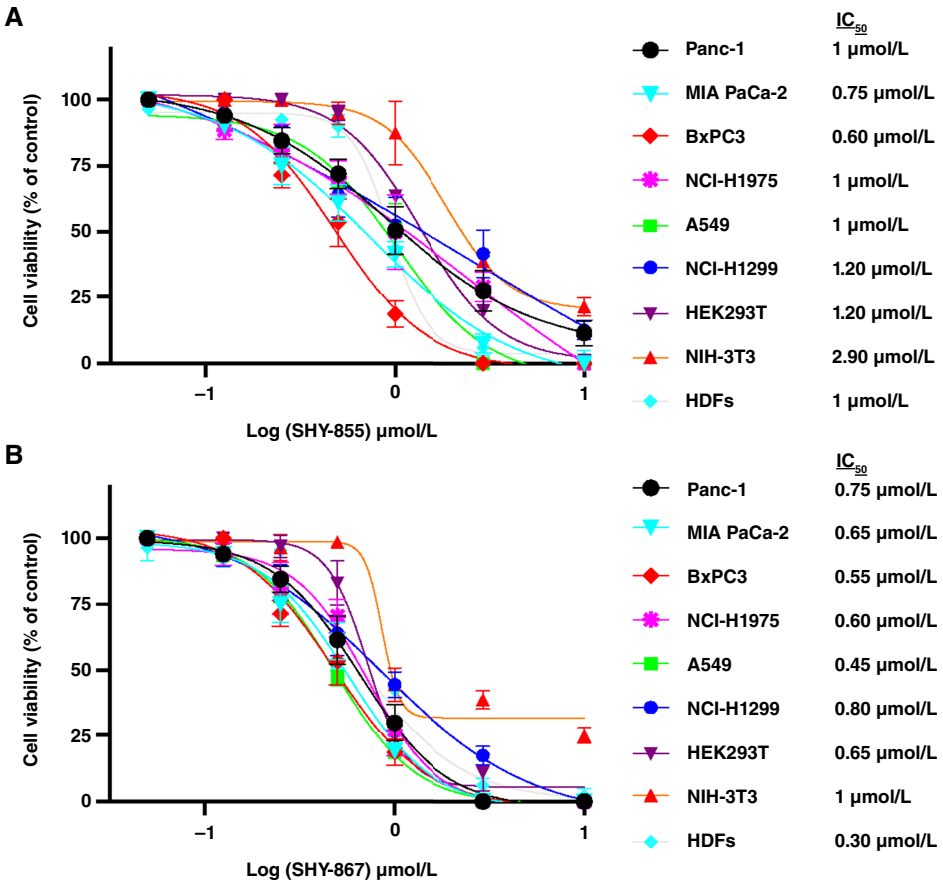

Figure 5.
Effects of compounds SHY-855 (**A**) and SHY-867 (**B**) on cellular proliferation. The indicated cell lines were incubated with compounds SHY-855 or SHY-867 for 72 hours with the indicated concentrations. Following 72 hours of incubation, cell viability was measured as described under "Materials and Methods". HDF, human dermal fibroblast.

here. They include the proteins studied and how they were prepared, the methods and materials used, the measurements made, and how the measurements were analyzed. Both previous publications studied H-Ras and the most recent K-Ras. The present study focused on K-Ras and several K-Ras mutants highly associated with different human tumors. The GTP-binding domains of H-Ras and K-Ras are quite similar but other segments of the proteins are distinct and their physiologic properties differ.

The greatest divergence between the results reported here and those reported in the previous publications are in the measured or calculated k_{off} values. Although k_{off} rates must be a consideration in developing a small-molecule GTP-binding competitor, we chose to focus on K_{on} rates for GTP binding to K-Ras because, biologically, GTP dissociation from K-Ras is intertwined with rates of the γ-phosphate hydrolysis and GDP dissociation, which in cells is mediated by guanine nucleotide exchange factor activity such as Son of Sevenless. How quickly GTP and K-Ras dissociate in a cell-free assay is not as physiologically relevant. Thus, we focused on k_{on} and K_d measurements in the SPA and filtration binding assays which yielded high calculated k_{off} rates. Problems with the earlier study measurements of k_{off}, to which the prior articles allude, may inevitably have led to the divergent K_d values.

Importantly, as described above, we have validated the conclusions that can be drawn from the 250 to 400 nmol/L K_d affinity data reported here—that is, that small-molecule inhibitors of GTP binding to WT K-Ras and several K-Ras mutants should be possible to discover—by identifying hundreds of them.

Numerous small-molecule therapeutics have been approved that target the ATP-binding sites of kinases (35, 36). None are approved or are in clinical trials that target the GTP-binding site of small GTPases such as K-Ras. It is interesting to consider our GTPase findings in the light of past kinase studies and kinase-targeted drug development. It is noteworthy that kinases and, based on our reported data, GTPases from the Ras superfamily exhibit similar affinity to nucleic acid cellular concentration ratios. The affinity of most kinases to ATP is about 1 to 100 µmol/L (37) and cellular ATP concentration is about 1 to 5 mmol/L (38); thus, the calculated ratio is in the range of 10^{-3} to 10^{-1}. We report affinity data for Ras to GTP of 200 to 400 nmol/L and cellular GTP concentrations in the range of 0.2 to 0.6 mmol/L (38), which yield a calculated ratio of approximately 10^{-3} in the range of the kinases.

Unlike kinase targets for which displacement of ATP by a small molecule is sufficient to block phosphorylation and activation events, to block Ras activation, antagonists targeting the GTP-binding site of Ras must both bind and induce or stabilize an inactive conformation, with similar effect to the GDP-bound inactive conformation of the GTPase. As blocking GTP binding in our cell-free assay cannot predict which conformation is induced by a compound, inhibitory activity also had to be assessed in cell- based assays. The demonstrated cell-based activity, including inhibition of MEK, Erk1/2, and Akt phosphorylation, Ras–GTP complex formation, and proliferation reported here demonstrate that the tested small molecules can penetrate tumor cells and induce or stabilize an inactive Ras conformation.

Analysis of the measured IC_{50} values of the two small molecules in the different assays indicates that they are most active in the

proliferation assays. In both cell-free competition assays and cell-based phosphorylation assays, the measured IC_{50} values are in the sub μmol/L range, whereas in the proliferation assays, they are in the high nmol/L range. These results may reflect the pan-Ras superfamily inhibitory effects of the molecules. In the proliferation assay, both compounds demonstrated the lowest inhibitory effects on NIH-3T3 cells which are the closest representative of normal cells. Similar results were also obtained for SHY-855 in human dermal fibroblasts; however, SHY-867 was very active in these cells (IC_{50} of 0.3 μmol/L). This suggests that SHY-855 is most likely less toxic and we have already incorporated this information in the design of our future compounds.

Recently developed small-molecule inhibitors targeting the K-Ras^{G12C} (15, 39–42) mutant, sotorasib and adagrasib, have been approved by the FDA. These inhibitors are different from the molecules described here. They are specific only to the K-Ras^{G12C} mutant, form covalent bonds with the free thiol group of the mutant, and are not competitive binders or blocker of the mutant protein in an inactive GDP-bound conformation. In practice, the vast majority of patients treated with these drugs have developed tumor resistance through many mechanisms, most of which are currently unknown (43). Considering the different mechanisms of action of the pan-K-Ras inhibitors described in this article, it is possible that they will not induce such acquired resistance and may overcome it in the clinic. Currently, there are additional K-Ras inhibitors in clinical development representing new therapeutic approaches, including emphasis on the "on" and "off" switch allele-specific and pan-RAS inhibition (44). However, none of them utilizes direct targeting of the GTP-binding site like the SHY compounds presented in this article.

Although further work remains to be done, this article strongly suggests that opportunities should exist to develop small-molecule therapeutics that address clear unmet medical needs such as cancer, fibrosis, and inflammatory conditions by directly targeting the GTP-binding site of K-Ras and other members of the Ras superfamily of small GTPases (45, 46).

Data Availability

The data generated in this study are available upon request from the corresponding author.

Authors' Disclosures

R. Hutcheson reports a patent for US 11,541,041 issued to SHY Therapeutics, LLC and a patent for US 17/414,565 pending to SHY Therapeutics, LLC. M.-J. Rudolph reports grants from SHY Therapeutics during the conduct of the study. C.H. Reynolds reports personal fees from SHY Therapeutics during the conduct of the study. T.M. Williams reports a patent for US17/414,565 pending and a patent for US 11,541,041 issued. M. Schmertzler reports a patent for US11,541,041 issued to SHY Therapeutics and a patent for US 17-414,565 pending to SHY Therapeutics. Y.R. Hadari reports a patent for US 11,541,041 issued to SHY Therapeutics, LLC and a patent for US 17/414,565 pending to SHY Therapeutics, LLC. No disclosures were reported by the other authors.

Authors' Contributions

L. Carta: Conceptualization, formal analysis, validation, investigation, writing–original draft, writing–review and editing. **R. Hutcheson:** Conceptualization, formal analysis, validation, investigation, writing–original draft, writing–review and editing. **C.L. Bigarella:** Conceptualization, formal analysis, validation, investigation, writing–original draft, writing–review and editing. **S. Zhang:** Conceptualization, formal analysis, validation, investigation, writing–original draft, writing–review and editing. **S.A. Davis:** Formal analysis, validation, investigation. **M.J. Rudolph:** Formal analysis, supervision, validation, investigation. **C.H. Reynolds:** Conceptualization, formal analysis, validation. **M. Quick:** Conceptualization, formal analysis, supervision, validation, investigation, writing–original draft, writing–review and editing. **T.M. Williams:** Conceptualization, formal analysis, supervision, validation, writing–original draft, writing–review and editing. **M. Schmertzler:** Conceptualization, formal analysis, writing–original draft, writing–review and editing. **Y.R. Hadari:** Conceptualization, formal analysis, supervision, validation, writing–original draft, writing–review and editing.

Acknowledgments

We dedicate this article in memory of L. Carta, our dear friend and colleague. This work was funded by SHY Therapeutics, LLC. We thank Allan S. Jacobson (University of Massachusetts, Worcester) for critical comments on the manuscript.

Note

Supplementary data for this article are available at Molecular Cancer Therapeutics Online (http://mct.aacrjournals.org/).

Received July 31, 2024; revised February 5, 2025; accepted August 19, 2025; posted first August 26, 2025.

References

1. Parker JA, Mattos C. The K-Ras, N-Ras, and H-Ras isoforms: unique conformational preferences and implications for targeting oncogenic mutants. Cold Spring Harb Perspect Med 2018;8:a031427.
2. Simanshu DK, Nissley DV, McCormick F. RAS proteins and their regulators in human disease. Cell 2017;170:17–33.
3. Stephen AG, Esposito D, Bagni RK, McCormick F. Dragging ras back in the ring. Cancer Cell 2014;25:272–81.
4. Milburn MV, Tong L, deVos AM, Brünger A, Yamaizumi Z, Nishimura S, et al. Molecular switch for signal transduction: structural differences between active and inactive forms of protooncogenic ras proteins. Science 1990;247:939–45.
5. Shieh JTC. Emerging RAS superfamily conditions involving GTPase function. PLoS Genet 2019;15:e1007870.
6. Hunter JC, Manandhar A, Carrasco MA, Gurbani D, Gondi S, Westover KD. Biochemical and structural analysis of common cancer-associated KRAS mutations. Mol Cancer Res 2015;13:1325–35.
7. Wennerberg K, Rossman KL, Der CJ. The Ras superfamily at a glance. J Cell Sci 2005;118:843–6.
8. Cox AD, Der CJ. Ras history: the saga continues. Small GTPases 2010;1:2–27.
9. Prior IA, Lewis PD, Mattos C. A comprehensive survey of Ras mutations in cancer. Cancer Res 2012;72:2457–67.
10. Hobbs GA, Der CJ, Rossman KL. RAS isoforms and mutations in cancer at a glance. J Cell Sci 2016;129:1287–92.
11. Pylayeva-Gupta Y, Grabocka E, Bar-Sagi D. RAS oncogenes: weaving a tumorigenic web. Nat Rev Cancer 2011;11:761–74.
12. Cox AD, Fesik SW, Kimmelman AC, Luo J, Der CJ. Drugging the undruggable RAS: mission possible? Nat Rev Drug Discov 2014;13:828–51.
13. Li S, Balmain A, Counter CM. A model for RAS mutation patterns in cancers: finding the sweet spot. Nat Rev Cancer 2018;18:767–77.
14. Jenkins RW, Sullivan RJ. NRAS mutant melanoma: an overview for the clinician for melanoma management. Melanoma Manag 2016;3:47–59.
15. McCormick F. Sticking it to KRAS: covalent inhibitors enter the clinic. Cancer Cell 2020;37:3–4.
16. Grapsa D, Syrigos K. Direct KRAS inhibition: progress, challenges and a glimpse into the future. Expert Rev Anticancer Ther 2020;20:437–40.
17. Feuerstein J, Kalbitzer HR, John J, Goody RS, Wittinghofer A. Characterisation of the metal-ion-GDP complex at the active sites of transforming and nontransforming p21 proteins by observation of the 17O-Mn superhyperfine coupling and by kinetic methods. Eur J Biochem 1987;162:49–55.
18. John J, Sohmen R, Feuerstein J, Linke R, Wittinghofer A, Goody RS. Kinetics of interaction of nucleotides with nucleotide-free H-ras p21. Biochemistry 1990;29:6058–65.

19. Jerabek-Willemsen M, Wienken CJ, Braun D, Baaske P, Duhr S. Molecular interaction studies using microscale thermophoresis. Assay Drug Dev Technol 2011;9:342–53.
20. Quick M, Javitch JA. Monitoring the function of membrane transport proteins in detergent-solubilized form. Proc Natl Acad Sci U S A 2007;104:3603–8.
21. Shi L, Quick M, Zhao Y, Weinstein H, Javitch JA. The mechanism of a neurotransmitter:sodium symporter–inward release of Na+ and substrate is triggered by substrate in a second binding site. Mol Cell 2008;30:667–77.
22. John J, Rensland H, Schlichting I, Vetter I, Borasio GD, Goody RS, et al. Kinetic and structural analysis of the Mg(2+)-binding site of the guanine nucleotide-binding protein p21H-ras. J Biol Chem 1993;268:923–9.
23. Goebel L, Kirschner T, Koska S, Rai A, Janning P, Maffini S, et al. Targeting oncogenic KRasG13C with nucleotide-based covalent inhibitors. Elife 2023;12:e82184.
24. Hadari YR, Schmertzler M, Williams TM, Carta L, Hutcheson R, Reynolds CH, inventors; SHY Therapeuticd LLC, assignee. Compounds that interact with the ras superfamily for the treatment of cancers, inflammatory diseases, rasopathies, and fibrotic disease. United States patent US-10940139-B2. 2020.
25. Zhang B, Zhang Y, Wang Z, Zheng Y. The role of Mg2+ cofactor in the guanine nucleotide exchange and GTP hydrolysis reactions of Rho family GTP-binding proteins. J Biol Chem 2000;275:25299–307.
26. Rouck JE, Krapf JE, Roy J, Huff HC, Das A. Recent advances in nanodisc technology for membrane protein studies (2012-2017). FEBS Lett 2017;591:2057–88.
27. Wu S, Liu B. Application of scintillation proximity assay in drug discovery. BioDrugs 2005;19:383–92.
28. Glickman JF, Schmid A, Ferrand S. Scintillation proximity assays in high-throughput screening. Assay Drug Dev Technol 2008;6:433–55.
29. Tucker J, Sczakiel G, Feuerstein J, John J, Goody RS, Wittinghofer A. Expression of p21 proteins in Escherichia coli and stereochemistry of the nucleotide-binding site. EMBO J 1986;5:1351–8.
30. Shih TY, Papageorge AG, Stokes PE, Weeks MO, Scolnick EM. Guanine nucleotide-binding and autophosphorylating activities associated with the p21src protein of Harvey murine sarcoma virus. Nature 1980;287:686–91.
31. Sigal IS, Gibbs JB, D'Alonzo JS, Temeles GL, Wolanski BS, Socher SH, et al. Mutant ras-encoded proteins with altered nucleotide binding exert dominant biological effects. Proc Natl Acad Sci U S A 1986;83:952–6.
32. Finkel T, Der CJ, Cooper GM. Activation of ras genes in human tumors does not affect localization, modification, or nucleotide binding properties of p21. Cell 1984;37:151–8.
33. Hara M, Tamaoki T, Nakano H. Guanine nucleotide binding properties of purified v-Ki-ras p21 protein produced in Escherichia coli. Oncogene Res 1988;2:325–33.
34. Manne V, Yamazaki S, Kung HF. Guanosine nucleotide binding by highly purified Ha-ras-encoded p21 protein produced in Escherichia coli. Proc Natl Acad Sci U S A 1984;81:6953–7.
35. Wang X, Wu X, Zhang A, Wang S, Hu C, Chen W, et al. Targeting the PDGF-B/PDGFR-β interface with destruxin A5 to selectively block PDGF-BB/PDGFR-ββ signaling and attenuate liver fibrosis. EBioMedicine 2016;7:146–56.
36. Roskoski R Jr. Properties of FDA-approved small molecule protein kinase inhibitors: a 2020 update. Pharmacol Res 2020;152:104609.
37. Knight ZA, Shokat KM. Features of selective kinase inhibitors. Chem Biol 2005;12:621–37.
38. Traut TW. Physiological concentrations of purines and pyrimidines. Mol Cell Biochem 1994;140:1–22.
39. Ostrem JM, Peters U, Sos ML, Wells JA, Shokat KM. K-Ras(G12C) inhibitors allosterically control GTP affinity and effector interactions. Nature 2013;503:548–51.
40. Canon J, Rex K, Saiki AY, Mohr C, Cooke K, Bagal D, et al. The clinical KRAS(G12C) inhibitor AMG 510 drives anti-tumour immunity. Nature 2019;575:217–23.
41. Hallin J, Engstrom LD, Hargis L, Calinisan A, Aranda R, Briere DM, et al. The $KRAS^{G12C}$ inhibitor MRTX849 provides insight toward therapeutic susceptibility of KRAS-mutant cancers in mouse models and patients. Cancer Discov 2020;10:54–71.
42. Lito P, Solomon M, Li L-S, Hansen R, Rosen N. Allele-specific inhibitors inactivate mutant KRAS G12C by a trapping mechanism. Science 2016;351:604–8.
43. Liu J, Kang R, Tang D. The KRAS-G12C inhibitor: activity and resistance. Cancer Gene Ther 2022;29:875–8.
44. Singhal A, Li BT, O'Reilly EM. Targeting KRAS in cancer. Nat Med 2024;30:969–83.
45. Qu L, Pan C, He S-M, Lang B, Gao G-D, Wang X-L, et al. The Ras superfamily of small GTPases in non-neoplastic cerebral diseases. Front Mol Neurosci 2019;12:121.
46. Prieto-Dominguez N, Parnell C, Teng Y. Drugging the small GTPase pathways in cancer treatment: promises and challenges. Cells 2019;8:255.